

# Ground State Phase Diagram of SU(3) $t$ - $J$ Chain

Junhao Zhang,<sup>1,\*</sup> Jie Hou,<sup>1</sup> Jie Lou,<sup>1,†</sup> and Yan Chen<sup>1,‡</sup>

<sup>1</sup>*Department of Physics and State Key Laboratory of Surface Physics, Fudan University, Shanghai 200433, China*  
(Dated: September 17, 2024)

Distinct from the SU(2) case, the fermionic systems with SU( $N$ ) symmetry are expected to exhibit novel physics, such as exotic singlet formation. Using the density matrix renormalization group technique, we obtain the ground state phase diagram of the SU(3)  $t$ - $J$  chain for density  $n < 1$ . The ground state phase diagram includes the Luttinger liquid, the extended Luther-Emery liquid characterized by a spin gap, and the phase separation state. We quantitatively assess the characteristics of the three phases by measuring spin gap, compressibility, various correlation functions and structure factors. We further study the extended Luther-Emery liquid phase and discover molecular superfluid quasi-long-range order. The mechanism of the molecular superfluid is the combination of three SU(3) fermions on sites that are not completely connected. Accordingly, we can speculate the behavior of the SU( $N$ )  $t$ - $J$  chain model with larger  $N$  values, operating within the same filling regime.

## I. INTRODUCTION

The mechanism of high- $T_c$  superconductivity and strongly correlated electron systems has attracted great interest in both theoretical and experimental studies[1, 2]. The two-dimensional  $t$ - $J$  model is generally considered a minimal model that captures the essential interplay between charge and spin degrees of freedom in cuprates[3]. It is the effective Hamiltonian of the Hubbard model in the limit of strong correlation. Meanwhile, the one-dimensional (1D)  $t$ - $J$  model exhibits several exciting properties. The ground state phase diagram of the 1D  $t$ - $J$  model was first demonstrated by M. Ogata *et al.* [4] theoretically and later verified by A. Moreno *et al.*[5] later with density matrix renormalization group (DMRG) algorithm. The phase diagram contains Luttinger liquid regions with the behavior of repulsive and attractive (i.e., superconducting) nature, spin gap, and phase separation for different values of  $J/t$ . The correlation functions and energy gaps determine their phase boundaries.

The spin freedom of electrons contains two spin components that expand the space carrying the fundamental representation of SU(2). A generalized symmetry SU( $N$ ) has been proposed in different fermionic systems. One of the most famous examples is the role SU(3) gauge symmetry playing in quantum chromodynamics[6, 7]. Recently, the theoretical exploration of the twisted bilayer graphene also leads to SU(4) symmetry for the multiple of electron spin and twofold valley degeneracy[8].

The development of quantum simulators provides a new approach to studying theoretical models through experimental measurements[9–12]. Ultracold Fermi gases of alkaline-earth isotopes, such as <sup>173</sup>Yb and <sup>87</sup>Sr, can carry multiple components with an intrinsic degree of freedom by their nuclear spins  $I$ . Interaction between atoms in optical lattices can be modulated by optical Feshbach resonance to have SU( $N$ ) symmetry. For relatively small values of  $N$ , SU( $N$ ) symmetry can be achieved by selecting nuclear spin states[13]. Moreover,

experimentalists have developed the ability to measure correlations in ultracold <sup>173</sup>Yb SU(6) Hubbard model in the Mott insulator regime[14, 15]. These advances shed light on exploring many-body physics with SU( $N$ ) symmetry. Systems with SU( $N$ ) symmetry instead of SU(2) spin symmetry may lead to the emergence of novel quantum phases and nontrivial physical behaviors.

The zero-temperature phase diagram of the 1D SU( $N$ ) Fermi-Hubbard model with  $N > 2$  has been investigated by various analytical and numerical techniques. The results are sketched for both incommensurate and commensurate fillings[29]. For incommensurate fillings, a metallic state shows up. Its physical property strongly depends on the sign of the coupling constant  $U$ . When  $U > 0$ , all modes are gapless, and a metallic Luttinger liquid phase emerges[30, 31]. On the other hand, a spin gap for SU( $N$ ) degrees of freedom develops in an attractive case ( $U < 0$ ). The charge density wave (CDW) or molecular superfluid (MS) instability dominates for high-density or low-density regimes. For commensurate fillings, the ground state tends to be  $p$ -merization with gapped charge mode and gapless spin mode when the filling equals  $1/p$  ( $p$ : integer).

The 1D SU( $N$ )  $t$ - $J$  model with a density below 1 (equivalence below  $1/N$  filling) is studied by P. Scholtzman[32] as an exactly solvable model at the supersymmetric line  $t = J$  with SU( $N|1$ ) symmetry. The global phase diagram of the 1D SU( $N$ )  $t$ - $J$  model away from the supersymmetric line has not been carefully studied. Whether the constraint on the local occupancy in strong coupling limit, which forbids the direct interaction between fermions of the number  $N$  ( $N > 2$ ), can break the emergence of the SU( $N$ ) singlet attracts our interests. At the particle density  $n = 1$ , SU( $N$ )  $t$ - $J$  chain model turns into 1D SU( $N$ ) Heisenberg model with the fundamental representation (represented by Young diagram  $\square$ ) on each site. It has been investigated theoretically by conformal field theory (CFT)[16, 17], known to belong to the universality class of the SU( $N$ )<sub>1</sub> Wess-Zumino-Witten(WZW) models with central charge  $c = N - 1$ [17–19]. It is known that the SU( $N$ )<sub>1</sub> WZW CFT describes the stable fixed point of the generic 1D gapless system with SU( $N$ ) symmetry. As an integrable model, the SU( $N$ ) Heisenberg chain was solved by Bethe Ansatz[20]. It has also been studied numerically by exact diagonaliza-

\* jhzhang16@fudan.edu.cn

† loujie@fudan.edu.cn

‡ yanchen99@fudan.edu.cn;

tion (ED)[21, 22], variational Monte Carlo[23], and DMRG methods[24–28].

In this paper, we determine the phase diagram of the SU(3)  $t$ - $J$  chain by examining the opening of spin gap and the divergence of compressibility. The correlation functions and their structure factors are studied numerically to sketch the characteristic behavior of each phase. These features are compared with SU(2) case[5] and 1D SU( $N$ ) Fermi-Hubbard model[29, 33] to distinguish the distinct phase in the phase diagram. We discover a quasi-long-range MS order of 3 fermions on different sites that are not fully connected. The region of the MS order phase occupied in the phase diagram is relatively small compared to the gapped superconducting region in the SU(2) case. It is compressed by less clustering energy gain and more fluctuation due to the more remarkable phase space of the singlet state.

Our paper is organized as follows. In Sec. II, we introduce the 1D SU(3)  $t$ - $J$  model and the setting of DMRG simulation. In Sec. III, we present the phase diagram and the identification of the phase boundary. In Sec. IV, we calculate the structure factor and compare it with its SU(2) counterpart. In Sec. V, the Luther-Emery liquid phase is further examined by calculating energy response and correlation functions. The summary and discussion are in the final Sec. VI.

## II. MODEL AND METHOD

In theoretical studies, SU( $N$ ) Hubbard model is usually mentioned to describe the alkaline earth atoms trapped in an optical lattice. The SU( $N$ ) generation of the Fermi-Hubbard model contains nearest-neighbor hopping and on-site interaction

$$H_{\text{Hubbard}}^{\text{SU}(N)} = -t \sum_{\langle i,j \rangle, \alpha} (c_{i\alpha}^\dagger c_{j\alpha} + \text{H.c.}) + \frac{U}{2} \sum_i n_i (n_i - 1), \quad (1)$$

where  $i, j$  labels chain sites,  $\alpha = 1, \dots, N$  is the SU( $N$ ) nuclear spin index. This model is invariant under the global  $U(1)$  symmetry, implying the conservation of the total number of atoms. Moreover, the SU( $N$ ) symmetry arises:  $c_{\alpha,i} \rightarrow \sum_\beta U_{\alpha\beta} c_{\beta,i}$ ,  $U$  being an SU( $N$ ) matrix. The actual symmetry group of the Fermi-Hubbard Hamiltonian is  $U(N) = U(1) \times \text{SU}(N)$ .

For the large  $U$  limit, the on-site repulsion confines the local state to two possible particle number occupation states around the average filling  $n$ :  $[n]$  and  $[n] + 1$ . In the same manner as the SU(2) case, the 1D SU( $N$ )  $t$ - $J$  model can be derived in second-order perturbation theory by projecting out the double occupancy states[49]

$$H_{t-J}^{\text{SU}(N)} = -t \sum_{\langle i,j \rangle, \alpha} \mathcal{P} (c_{i\alpha}^\dagger c_{j\alpha} + \text{H.c.}) \mathcal{P} + J \sum_{\langle i,j \rangle, \lambda} (\mathbf{T}_i^{\lambda\dagger} \mathbf{T}_j^\lambda - \gamma n_i n_j), \quad (2)$$

where  $\mathbf{T}_i^{\lambda\dagger}$  and  $\mathbf{T}_i^\lambda$  with  $\lambda = 1, \dots, N^2 - 1$  denote the SU( $N$ ) spin operators and their Hermite conjugates. They get their

explicit expression from the SU( $N$ ) Lie algebra generators. In the fermion case, the local state space is described by those antisymmetric representations of the SU( $N$ ) group. For instance, when the average local density  $n$  satisfies  $n < 1$ , the local degree of freedom is described by the direct sum of the trivial hole (*singlet*) and the  $N$ -dimensional fundamental, irreducible representation of SU( $N$ ) ( $\square$ ). The coefficient  $\gamma$  in the interaction term depends on the choice of generator basis. We choose the interaction Hamiltonian in a simple form with zero trace

$$H_{t-J}^{\text{SU}(N)} = -t \sum_{\langle i,j \rangle, \alpha} \mathcal{P} (c_{i\alpha}^\dagger c_{j\alpha} + \text{H.c.}) \mathcal{P} + J \sum_{\langle i,j \rangle, \alpha, \beta} (c_{i\alpha}^\dagger c_{i\beta} c_{j\beta}^\dagger c_{j\alpha} - n_{i\alpha} n_{j\beta}), \quad (3)$$

where the interaction term is consistent with the usual form

$$H_J^{\text{SU}(N)} = J \sum_{i,j} \frac{1}{2} \left( P_{ij} - \frac{1}{N} \right), \quad (4)$$

with 2-site permutation operator  $P_{ij}$  exchange the state on site  $i, j$ .

We use the DMRG algorithm to study SU(3)  $t$ - $J$  chain with open boundary condition and the length up to  $L = 120$  sites. The DMRG algorithm conserves the total particle number  $N_{\text{tot}} = nL$ , set to multiples of 3 to maintain color neutrality. We extrapolate the thermodynamic limit by calculating systems of size  $L = 30, 60, 90$ . These calculations use the ITensor library[34] DMRG update, keeping the bond dimension  $m$  up to 5,000. The maximum truncation error of ground state DMRG simulation was of order  $10^{-8}$ . At least 100 sweeps are done for all density and interaction settings.

We calculated the energy gap to SU(3) spin-flip excitations to characterize the phases and find the phase boundaries. Several kinds of correlation functions are also calculated to describe the different phases, such as the density-density correlation function,

$$N_{ij} = \langle n_i n_j \rangle - \langle n_i \rangle \langle n_j \rangle. \quad (5)$$

The SU(3) spin-spin correlation function is calculated as

$$T_{ij} = \sum_{\lambda=1}^{N^2-1} (\langle \mathbf{T}_i^\lambda \mathbf{T}_j^\lambda \rangle - \langle \mathbf{T}_i^\lambda \rangle \langle \mathbf{T}_j^\lambda \rangle), \quad (6)$$

where  $\mathbf{T}^\lambda$  are chosen to be Hermite generator of the fundamental representation. It is necessary to write down the explicit form of  $T^3$  and  $T^8$

$$T^3 = \frac{1}{2} \begin{pmatrix} 1 & 0 & 0 \\ 0 & -1 & 0 \\ 0 & 0 & 0 \end{pmatrix}, T^8 = \frac{1}{2\sqrt{3}} \begin{pmatrix} 1 & 0 & 0 \\ 0 & 1 & 0 \\ 0 & 0 & -2 \end{pmatrix}. \quad (7)$$

These two SU(3) spin components are the two diagonal matrices of Gell-Mann Matrices. They are orthogonal to the density channel. The corresponding structure factors of a certain two-point correlation  $X_{ij}$  are obtained by a Fourier transformation

$$X(k) = \frac{1}{L} \sum_{i,j=1}^L e^{ik(x_i - x_j)} X_{ij}. \quad (8)$$

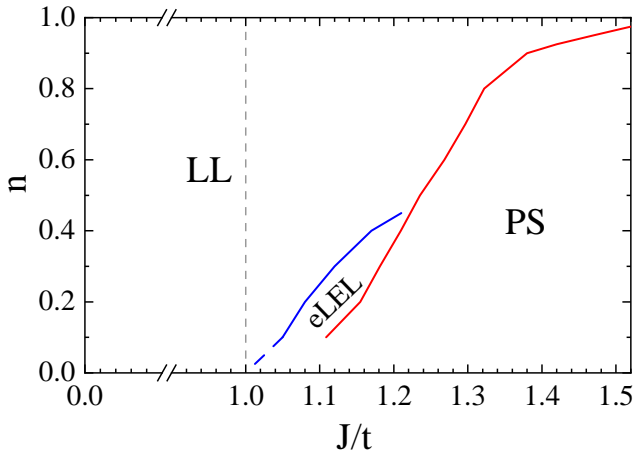


FIG. 1. Phase diagram of the 1D SU(3)  $t$ - $J$  model from DMRG for densities  $0.1 \leq n \leq 0.95$  and in the range  $0 < J/t \leq 1.5$ , where  $n = N/L$  is the particle density. The grey dashed line  $J = t$  is the exactly solvable parameter regime.

Even though the system we calculated lacks translational invariance for the open boundary conditions, the effect of finite size could hardly be observed in the Fourier transformation procedure.

### III. PHASE DIAGRAM

The phase diagram for the SU(3)  $t$ - $J$  model (FIG. 1.) contains 3 phases: Luttinger liquid(LL), a spin-gapped phase named extended Luther-Emery liquid(LEL), and phase separation (PS). It differs from the phase diagram of SU(2) case mainly in the position of the phase boundary.

#### A. Luttinger Liquid

We can characterize this phase through the value of the Luttinger parameter  $K_\rho$ , with  $K_\rho < 1$  for a repulsive interaction on the density sector,  $K_\rho = 1$  and  $K_\rho > 1$  for the free and attractive case. We obtain the structure factor for the density correlation to compute  $K_\rho$ .  $N(k)$  does not show qualitative difference from the SU(2) case. They both show a linear behavior with a slope proportional to  $K_\rho$  in  $k \rightarrow 0$  limit[30, 35–37]

$$N(k \rightarrow 0) \rightarrow \frac{NK_\rho |k| a}{2\pi}. \quad (9)$$

where  $a$  is the lattice constant. It can be derived from the Fourier transformation of the inverse quadratic term of the asymptotic density correlation[37].

$$N_{r,0} \sim n^2 - \frac{NK_\rho}{2(\pi r)^2} + A_1 \frac{\cos(2k_F r)}{r^{2K_\rho/N+2-2/N}}. \quad (10)$$

By calculating density structure factors for different  $n$  and  $J$ , we find that  $K_\rho \rightarrow 1/3$  when  $J \rightarrow 0$  for any densities below

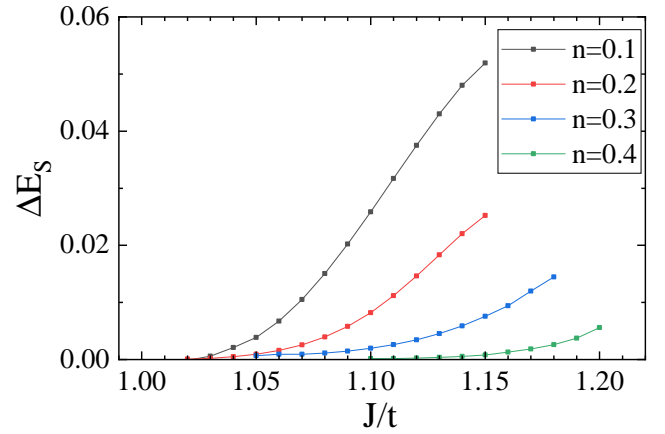


FIG. 2. Spin gap  $\Delta E_S$  in the thermodynamic limit as a function of  $J = 0.8 - 1.3$  for different  $n$ . It is extrapolated by finite-size scaling.

1, which results from the same slope 0.5 as in SU(2) case. The physical property of density, spin correlations, and corresponding structure factors is further discussed in Sec. IV A.

#### B. Spin-Gap Phase

As  $J$  increases, the value of  $K_\rho$  grows more significant than 1, and the system gets into the attractive phase. Meanwhile, a spin gap appears in a low-density region.

The spin gap  $\Delta E_S$  is measured directly to find the spin gap region. It is defined as the spin excitation energy from a singlet to a spin-flipped state, which is the energy difference

$$\Delta E_S = E_0(N, T_{tot}^3 = 1, T_{tot}^8 = 0) - E_0(N, T_{tot}^3 = 0, T_{tot}^8 = 0), \quad (11)$$

where the subscript 0 means the lowest-energy level with given quantum numbers  $N$ ,  $T_{tot}^3$ , and  $T_{tot}^8$ . We extrapolate the spin gap of different finite system sizes to the thermodynamic limit with  $L = 30, 60, 90$ , and  $120$ . The spin excitation energy vs.  $1/L$  at  $n = 0.1$  to  $0.4$  for various values of  $J$  is presented in Fig. 2. The extrapolations to the thermodynamic limit are performed with 2nd-order polynomials in FIG. 2. The extrapolations show that for  $J = 1.0t$ , the gap extrapolates to zero and that for  $J = 1.2t$ , a finite gap emerges.

This calculation is performed for different densities  $n$  and  $J$  to obtain the region with a spin gap in FIG. 2. A finite spin gap is observed when  $J$  increases more remarkably than the supersymmetric value  $J = 1.0t$ . We defined the phase boundary in the phase diagram (FIG. 1) as the value of  $J$  for which  $\Delta E_S > 10^{-3}t$ . The spin gap implies the existence of the regime where pairs or trions form. A more detailed discussion of the pairing mechanics is addressed in Sec. V.

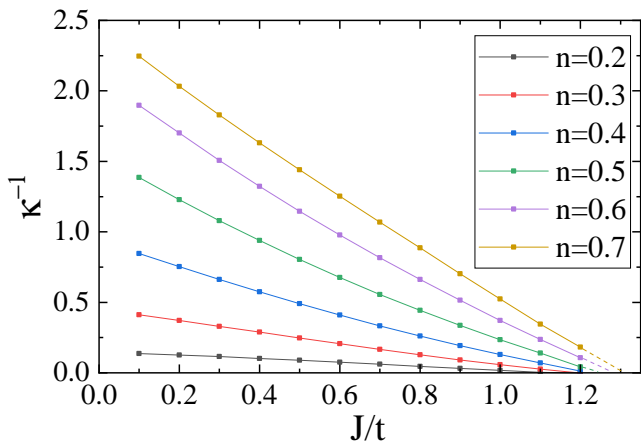


FIG. 3. Inverse of the compressibility  $\kappa^{-1}$  as a function of  $J$  for different density.

### C. Phase Separation

As the interaction  $J$  grows, the attraction among the particles would be so strong that particles start to form SU(3) anti-ferromagnetic domains. The system is separated into particle-rich and hole-rich regions. It is the same as SU(2) case that all particles condensate in a single island in  $J \rightarrow \infty$  limit. This phase is called the electron solid phase, proposed by Chen and Moukouri[38]. The effect of the kinetic term is strongly suppressed while the spin fluctuations can be described by SU(3) Heisenberg model. The divergence of compressibility is considered to detect this phase. We calculate the inverse of the compressibility, which should vanish at the threshold of the phase separation.

The expression for the ground state inverse compressibility is given by

$$\begin{aligned} \kappa^{-1}(n) &= n^2 \frac{\partial^2 e_0(n)}{\partial n^2} \\ &\approx n^2 \frac{[e(n + \Delta n) + e(n - \Delta n) - 2e(n)]}{\Delta n^2}, \end{aligned} \quad (12)$$

where  $e_0(n) = E_0/L$  is the energy per site, and the second line shows the approximation for practical numerical calculation when the change in the density is finite. FIG. 3 shows  $\kappa^{-1}$  versus  $J/t$  for different densities. We can locate the boundary of the phase-separated phase by finding the critical value  $J_c(n)$  where  $\kappa^{-1}$  vanishes.

## IV. CORRELATION FUNCTIONS

### A. Structure Factors

The phase diagram of the 1D SU(3)  $t$ - $J$  model looks distorted with respect to the SU(2) case. Nevertheless, we discover significant deviations in correlation functions. The structure factors for certain correlation functions provide a

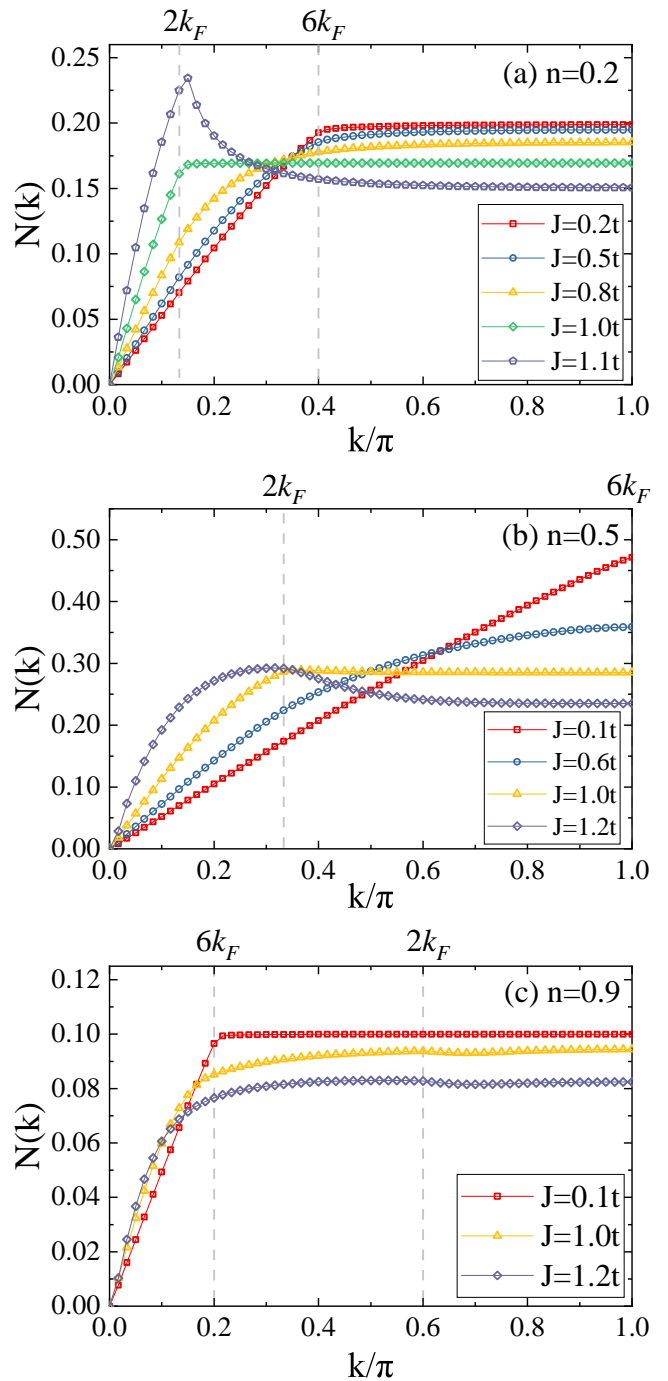


FIG. 4. Structure factor  $N(k)$  for density-density correlation function for  $L = 120$  and for different values of  $n$  and  $J$ . The location of  $6k_F$  is determined by folding them back to the outer sector in the first Brillouin zone.

more detailed characterization of the different phases. They are displayed in FIG. 4-5.

FIG. 4 shows the structure factor  $N(k)$  for the density-density correlation function. We plot several values of  $J$  for  $n = 0.2, 0.5,$  and  $0.9$ . We can see  $N(k = 0) = 0$  due to the conservation of total particle numbers for all cases. Similarly,

all cases show linear behavior for  $k \rightarrow 0$ , implying the gapless feature in the charge sector.

For  $J \ll t$ , the ground state is a repulsive LL phase. A  $6k_F$  ( $k_F^{\text{SU}(3)} = n\pi/3$ ) anomaly can be observed, which is different from the typical  $4k_F$  ( $k_F^{\text{SU}(2)} = n\pi/2$ ) anomaly in SU(2)  $t$ - $J$  model and not be reflected in Eq.14. The two anomalies locate at the same wave vectors when we express them in the manner of density  $n$  ( $6k_F^{\text{SU}(3)} = 4k_F^{\text{SU}(2)} = 2n\pi$ ). They correspond precisely to a charge modulation with a spatial distance periodicity between the electrons. Due to the repulsive between electrons, they form a 1D equivalent of a Wigner crystal[30, 39, 40]. In 1D, Wigner crystallization occurs in all densities for the long-range nature of the Coulomb potential. Meanwhile, the quantum fluctuation breaks the long-range order in 1D[30]. For these reasons, we expect a slight anomaly at  $2Nk_F$  on the density structure factor of the 1D SU( $N$ )  $t$ - $J$  model. This is different from the ones in SU( $N$ ) Fermi-Hubbard model because double occupancy is forbidden in  $t$ - $J$  model.

Like the SU(2) case, as  $J$  increases, the  $6k_F$  anomaly is suppressed, and a  $2k_F$  apex is formed. It marks a  $2k_F$  charge-density-wave, corresponding to the pairing charge-density wave with  $2k_F$  in SU(2) case. However, when we consider the wavelength written in density

$$\lambda = \frac{2\pi L}{2k_F} = \frac{3L}{n}, \quad (13)$$

it shows three times the distance of a single particle lattice, signaling the 3-fermion pairing in a wavelet. In the attracting regime, fermions combine together in a different method compared with the SU(2) pairing method. This support that the singlet formation of 3 spins still dominates the attractive zone despite the less connection between spins in  $t$ - $J$  model. By comparing different densities, we observe the  $2k_F$  apex suppressed as particle density increases, which signals weaker 3-clustering in the density channel for higher density. The peaks and anomalies are slightly more prominent than  $2k_F$  and  $6k_F$  in the  $N(k)$  diagram. It results from the open boundary condition of our DMRG simulation. The local density is suppressed near the boundaries, so the effective density is larger than the total charge and system size ratio.

In FIG. 5, the structure factor  $T(k)$  for the spin-spin correlation function is shown. For  $J < t$  at all densities, the tendency to antiferromagnetism is revealed by observing a peak at  $2k_F$ . It results from the quasi-long-range SU(3) antiferromagnetic order. The slopes near  $k \rightarrow 0$  limit remain almost unchanged in repulsive region. It is consistent with the quadratic term in asymptotic spin correlation function in repulsive Luttinger liquid.

$$T_{r,0} \sim -\frac{1}{2(\pi r)^2} + B_1 \frac{\cos(2k_F r)}{r^{2K_p/N+2-2/N}}. \quad (14)$$

As  $J$  increases, the peak is suppressed, implying the existence of molecular superfluid phase. The spin gap develops in low density, signaling a phase like the LEL phase with the singularity at  $2k_F$  completely suppressed. This covers the MS phase regimes. It shares some behaviors with the typical LEL phase,

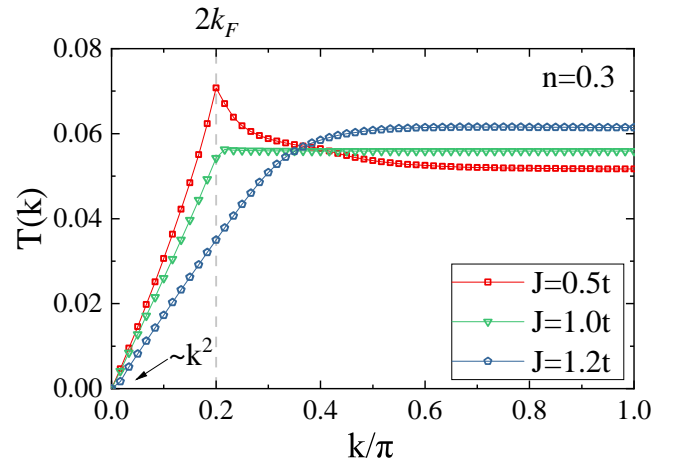


FIG. 5. Structure factor  $T(k)$  for SU(3) spin-spin correlation function for  $L = 120$  and for different values of  $n$  and  $J$ .

such as exponential decay of the spin-spin correlation function and the quadratic behavior at small  $k$ 's in the structure factor.

## V. TRION AND EXTENDED LEL PHASE

The peaks of FIG. 4 at  $2k_F$  and the suppressed anomaly in FIG. 5 imply the existence of a 3-clustering phase. Fundamental representations cluster into singlets when  $J$  increases. This clustering should be weaker than the pairing because the interaction forming singlet cannot link 3 SU(3) particles to each other. The strong fluctuation in the 1D system may break the long-range clustering order with higher translational symmetry breaking. For the  $t$ - $J$  model, A. Seidel *et al.* proved that the energy spin-gapped SU(2)-invariant Luttinger liquids have  $hc/2e$  flux periodicity for the broken translational symmetry with a doubling of the unit cell[41, 42]. To reveal the 3-clustering state, we calculate the energy dependence on the flux in the periodic boundary condition

$$H(\Phi) = -t \sum_{\langle i,j \rangle, \alpha} \mathcal{P} \left( e^{(2\pi i/L)\Phi/\Phi_0} c_{i\alpha}^\dagger c_{j\alpha} + H.c. \right) \mathcal{P} + H_J, \quad (15)$$

in spin-gap opening region ( $n = 0.1, J = 1.0-1.1t$ ).  $\Phi_0 \equiv hc/e$  is the elementary flux quantum. We observe a branch of quadratic ground state energy spectrum declining as  $J$  increases, referring to  $E_0(\Phi = \Phi_0/2)$ . The gap between bottoms of quadratic spectrums will close when  $J$  exceeds  $1.10t$ , resulting in a  $\Phi_0/3$  periodicity. By analogy, this indicates the combination of trion carriers with the  $\Phi_0/2$  periodicity for the superconducting phase in the SU(2) case.

This periodicity has also been studied by W.J. Chetcuti *et al.* [43, 44]. They observe the same behavior from small  $U$  to large  $U$  in SU(3) Fermi-Hubbard model with flux penetrating the ring for incommensurate fillings. This shows the paramagnetic persistent current behavior, which supports the 3-clustering mechanism at the mesoscopic scale.

The  $N$ -clustering feature fits the characteristics of the MS phase in 1D SU( $N$ ) Fermi-Hubbard model with  $N > 2$  [29].

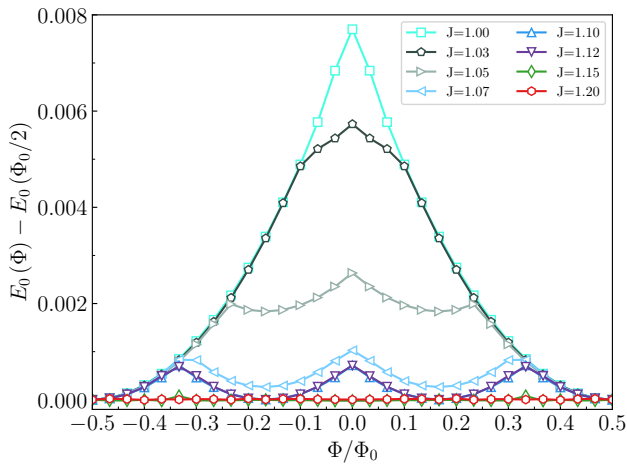


FIG. 6. Ground state energy  $E_0(\Phi)$  with respect to  $E_0(\Phi_0/2)$  for SU(3)  $t$ - $J$  flux model (Eq. 15). The data of negative  $\Phi$  is copied from its positive counterpart for the parity symmetry.

For  $U < 0$  region, the LEL phase is discovered at sufficiently low density. The superfluid instability is a molecular one with the order parameter  $M_i = c_{i,1}^\dagger c_{i,2}^\dagger \cdots c_{i,N}^\dagger$ . This corresponds to the formation of SU( $N$ ) singlet by  $N$  fermions on a single site. This phase with  $U < 0$  is governed by the competition between the CDW and molecular superfluid (MS) orders.

In SU(3)  $t$ - $J$  model, the local singlet is forbidden by the occupation constraint, so the clustering order is defined on three adjacent sites

$$C(i) = \frac{1}{\sqrt{6}} \sum_{\alpha,\beta,\gamma=1}^3 \varepsilon^{\alpha\beta\gamma} c_{i,\alpha} c_{i+1,\beta} c_{i+2,\gamma}, \quad (16)$$

where  $\varepsilon^{\alpha\beta\gamma}$  is the antisymmetric tensor. We compare the correlation function of clustering order

$$C(x) = \langle C(i) C^\dagger(i+x) \rangle, \quad (17)$$

with the correlation of pairing order,

$$\Delta^\alpha(x) = \langle \Delta^\alpha(i) \Delta^{\alpha\dagger}(i+x) \rangle, \quad (18)$$

where  $\Delta^\alpha(i) = \sum_{\beta,\gamma} \varepsilon^{\alpha\beta\gamma} c_{i,\beta} c_{i+1,\gamma}$ , and CDW correlation

$$N(x) = \langle N_{i,i+x} \rangle. \quad (19)$$

Fig. 7(a) shows the decay of density-density and MS correlation in real space. The upper envelope curves of both correlation functions suggest that they decay as the power law when the wave part is removed. The less decaying rate shows that the CDW quasi-long-range order dominates in the LL regime. FIG. 7(b) shows the behavior of the three correlation functions for the LEL phase. We can observe that the envelope curve of the singlet clustering correlation function shows the power law decay behavior. The 3-clustering order decays slower than the pairing and CDW orders, regarded as the dominant order. The asymptotic form of the correlation functions is

$$N(x) \sim \cos(2k_F x) x^{-\alpha_N}, \quad (20)$$

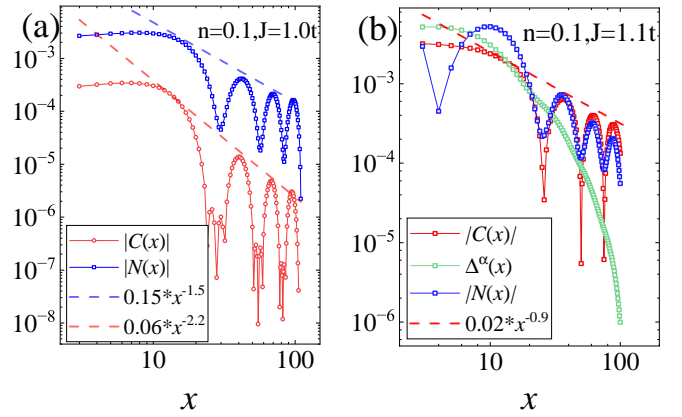


FIG. 7. MS  $|C(x)|$ , pairing  $\Delta^\alpha(x)$  and density  $N(x)$  correlation functions in LL (a) and LEL (b) phase. The upper envelope line shows the algebraic decay of corresponding correlation functions.

$$C(x) \sim \sin(k_F x) x^{-\alpha_C}. \quad (21)$$

Comparing the two correlation function diagrams, we find that the MS order becomes more substantial when the spin gap opens than the CDW order. Due to the dominant MS order, the  $hc/3e$  flux periodicity, and the finite spin gap, we describe this phase as the extended LEL phase.

We calculate the exponent's dependence with  $J$  and plot them with the energy difference between two quadratic branches  $\Delta E_\Phi$  and the spin gap  $\Delta E_S$  in FIG. 8. These variables show signals of phase transition in the range  $J/t \in (1.05, 1.10)$ . The power law exponents show significant distinction with that of in the attractive Fermi-Hubbard model, which is  $\alpha_N^{FH} = 2K_\rho/N$  and  $\alpha_C^{FH} = (K_\rho + N^2/K_\rho)/(2N)$  (odd  $N$ ) [45–47]. They do not satisfy this relationship quantitatively, implying the distinct features in this MS state. Furthermore, the exponent of MS correlation declines to below 1, the minimum value of  $\alpha_C^{FH}$ , which means a more robust MS order than in the Fermi-Hubbard model. This inconsistency is more apparent in the SU(3)  $t$ - $J$  model than in its SU(2) counterpart. No lower bound is greater than 0 in the MS component for even  $N$ ,  $\alpha_C^{FH} = N/2K_\rho$ . The more extensive phase space occupation of singlets is proposed to extend the correlation range of the MS order. The explicit relation to the Luttinger parameter  $K_\rho$  may need more precise calculation by bosonization.

The above numerical results supports the existence of the string-linked singlet simplex in the SU( $N$ ) fermion model [48]. This simplex has higher energy than the loop-like ones or more highly-linked ones. It could be explained by the effect of one-dimensional systems extending the effective interaction range.

## VI. SUMMARY AND DISCUSSION

In this work, we calculate the phase diagram of the 1D SU(3)  $t$ - $J$  model numerically by DMRG. The phase boundary of three phases: Luttinger liquid, extended Luther-Emery

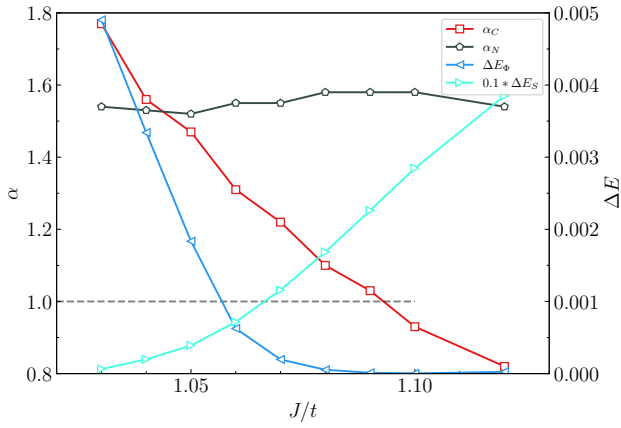


FIG. 8. 3-clustering exponent  $\alpha_C$ , density correlation  $\alpha_N$ , energy difference between two quadratic branches  $\Delta E_\Phi = E_0(\Phi = 0) - E_0(\Phi = \Phi_0/3)$  in ring model(15) and spin gap  $\Delta E_S$  (multiplied by 0.1 to fit scale).

liquid, and phase separation are demonstrated. We compare the result with the thoroughly studied  $SU(2)$   $t$ - $J$  model. For density-density correlation, we find the constant  $2k_F$  and  $6k_F$

singularity in its structure factor, which results from CDW instability and tendency to Wigner crystallization. We predict the  $2k_F$  and  $2Nk_F$  singularity for 1D  $SU(N)$   $t$ - $J$  model in the same filling regime.

We further characterize the extended LEL phase for its novel clustering structure through persistent currents and correlation functions. It is confirmed that three fundamental irreducible representations form a singlet in line under antiferromagnetic interaction. They differ from the on-site molecular superfluid singlet in the  $SU(N)$  attractive Fermi-Hubbard model in the space structure. This feature may affect ground state properties, leading to different power law exponents for density and MS correlation.

## ACKNOWLEDGMENTS

This work is supported by the National Key Research and Development Program of China (Grant No. 2022YFA1404204) and the National Natural Science Foundation of China (Grants Nos. 11625416 and 12274086). The authors acknowledge Beijing PARATERA Tech CO., Ltd. (<https://www.paratera.com/>) for providing HPC resources that have contributed to the numerical results reported in this paper.

- 
- [1] J. G. Bednorz, K. A. Müller, *Zeitschrift für Physik B Condensed Matter* **64**, 189 (1986).
- [2] P. W. Anderson, *Science* **235**, 4793 (1987).
- [3] F. C. Zhang and T. M. Rice, *Phys. Rev. B* **37**, 3759 (1988).
- [4] M. Ogata, M. U. Luchini, S. Sorella, and F. F. Assaad, *Phys. Rev. Lett.* **66**, 2388 (1991).
- [5] A. Moreno, A. Muramatsu, and S. R. Manmana, *Phys. Rev. B* **83**, 205113 (2011).
- [6] D. J. Gross and F. Wilczek, *Phys. Rev. Lett.* **30**, 1343 (1973).
- [7] H. D. Politzer, *Phys. Rev. Lett.* **30**, 1346 (1973).
- [8] N. F. Q. Yuan and L. Fu, *Phys. Rev. B* **98**, 045103 (2018).
- [9] I. Bloch, J. Dalibard, and S. Nascimbène, *Nature Physics* **8**, 267 (2012).
- [10] I. Bloch, *Nature Physics* **1**, 23 (2005).
- [11] R. Zhang, Y. Cheng, P. Zhang, and H. Zhai, *Nature Reviews Physics* **2**, 213 (2020).
- [12] R. Blatt and C. F. Roos, *Nature Physics* **8**, 277 (2012).
- [13] D. Tusi, L. Franchi, L. F. Livi, K. Baumann, D. B. Orenes, L. Del Re, R. E. Barfknecht, T. Zhou, M. Inguscio, G. Cappellini, M. Capone, J. Catani, and L. Fallani, *Nature Physics* **18**, 1201 (2022).
- [14] S. Taie, R. Yamazaki, S. Sugawa, and Y. Takahashi, *Nature Physics* **8**, 825 (2012).
- [15] S. Taie, E. Ibarra-García-Padilla, N. Nishizawa, Y. Takasu, Y. Kuno, H. T. Wei, R. T. Scalettar, K. R. Hazzard, and Y. Takahashi, *Nature Physics* **18**, 1356 (2022).
- [16] C. Itoi, S. Qin, and I. Affleck, *Phys. Rev. B* **61**, 6747 (2000).
- [17] I. Affleck, *Nuclear Physics B* **265**, 409 (1986), *Nuclear Physics B* **305**, 582 (1988).
- [18] V. Knizhnik and A. Zamolodchikov, *Nuclear Physics B* **247**, 83 (1984).
- [19] P. Di Francesco, P. Mathieu, and D. Sénéchal, *Conformal field theory*, (Springer, New York, 1997).
- [20] B. Sutherland, *Phys. Rev. B* **12**, 3795 (1975).
- [21] P. Nataf and F. Mila, *Phys. Rev. B* **93**, 155134 (2016).
- [22] K. Wan, P. Nataf, and F. Mila, *Phys. Rev. B* **96**, 115159 (2017).
- [23] D. Vörös and K. Penc, *Phys. Rev. B* **104**, 184426 (2021).
- [24] P. Nataf and F. Mila, *Phys. Rev. B* **97**, 134420 (2018).
- [25] M. Führinger, S. Rachel, R. Thomale, M. Greiter, and P. Schmitteckert, *Annalen der Physik* **12**, 922-936 (2008).
- [26] P. Fromholz, S. Capponi, P. Lecheminant, D. J. Papoular, and K. Totsuka, *Phys. Rev. B* **99**, 054414 (2019).
- [27] S. Gozel, P. Nataf, and F. Mila, *Phys. Rev. Lett.* **125**, 057202 (2020).
- [28] P. Nataf, S. Gozel, and F. Mila, *Phys. Rev. B* **104**, L180411 (2021).
- [29] S. Capponi, P. Lecheminant, and K. Totsuka, *Annals of Physics* **367**, 50 (2016).
- [30] T. Giamarchi, *Quantum physics in one dimension*, The international series of monographs on physics No. 121 (Clarendon ; Oxford University Press, Oxford : New York, 2004).
- [31] A. O. Gogolin, A. A. Nersisyan, and A. M. Tsvelik, *Bosonization and strongly correlated systems* (Cambridge University Press, 1998).
- [32] P. Schlottmann, *J. App. Phys.* **73**, 6645 (1993).
- [33] R. Assaraf, P. Azaria, M. Caffarel, and P. Lecheminant, *Phys. Rev. B* **60**, 2299 (1999).
- [34] M. Fishman, S. R. White, and E. M. Stoudenmire, *SciPost Phys. Codebases* **4** (2022).
- [35] R. T. Clay, A. W. Sandvik, and D. K. Campbell, *Phys. Rev. B* **59**, 4665 (1999).
- [36] S. Ejima, F. Gebhard, and S. Nishimoto, *Europhysics Letters (EPL)* **70**, 492 (2005).

- [37] S. R. Manmana, K. R. A. Hazzard, G. Chen, and A. M. Rey, *Phys. Rev. A* **84**, 043601 (2011).
- [38] L. Chen and S. Moukouri, *Phys. Rev. B* **53**, 1866 (1996).
- [39] G. D. Mahan, *Many-particle physics*, 3rd ed., (Kluwer Academic/Plenum Publishers, 2000).
- [40] E. Wigner, *Phys. Rev.* **46**, 1002 (1934).
- [41] A. Seidel and D.-H. Lee, *Phys. Rev. Lett.* **93**, 046401 (2004).
- [42] A. Seidel and D.-H. Lee, *Phys. Rev. B* **71**, 045113 (2005).
- [43] W. J. Chetcuti, T. Haug, L.-C. Kwek, and L. Amico, *SciPost Phys.* **12**, 033 (2022).
- [44] W. J. Chetcuti, J. Polo, A. Osterloh, P. Castorina, and L. Amico, *Commun. Phys.* **6**, 128 (2023).
- [45] P. Lecheminant, E. Boulat, and P. Azaria, *Phys. Rev. Lett.* **95**, 240402 (2005).
- [46] P. Lecheminant, P. Azaria, and E. Boulat, *Nuclear Physics B* **798**, 443 (2008).
- [47] S. Capponi, G. Roux, P. Lecheminant, P. Azaria, E. Boulat, and R. White, *Phys. Rev. A* **77**, 013624 (2008).
- [48] D. P. Arovas, *Phys. Rev. B* **77**, 104404 (2008).
- [49] J. C. He and Y. Chen, *Phys. Rev. B* **105**, 245117 (2022).